PNE-1001
C. 2

PNE 1001

GASBUGGY PRESHOT SUMMARY REPORT

FRED HOLZER, EDITOR

Lawrence
Radiation
Laboratory
Livermore

PLOWSHARE

UNITED STATES ATOMIC ENERGY COMMISSION

CIVIL, INDUSTRIAL AND SCIENTIFIC USES FOR NUCLEAR EXPLOSIVES

29664

Printed in USA. Price $3.00. Available from the Clearinghouse for Federal Scientific and Technical Information, National Bureau of Standards, U. S. Department of Commerce, Springfield, Virginia 22151.

TID-4500, UC-35
Nuclear Explosions —
Peaceful Applications

PNE-1001

GASBUGGY PRESHOT SUMMARY REPORT

Fred Holzer, editor

Lawrence Radiation Laboratory
Livermore, California

November 1967

CONTENTS

GASBUGGY PRESHOT SUMMARY REPORT

ABSTRACT

As part of the Gasbuggy preshot work, two holes, GB-1 and GB-2, were drilled and completed naturally approximately 190 and 300 feet, respectively, from the explosive-emplacement hole, GB-E.

The Pictured Cliffs sandstone, extending from 3916 to 4202 ft below the surface, has the following average properties: bulk density, 2.47 g/cm^3; compressional velocity, 13,500 ft/sec; porosity, 10%; and water saturation, 58% (4 to 5% water content by weight). The total gas in place is calculated to be 5.8 billion cubic feet (bcf) per 160 acres. When zones having water saturations of 60% or more are eliminated, a net volume of 4.7 bcf is obtained. While core permeabilities average 0.16 md, indicated in-situ permeabilities from buildup tests are between 0.01 and 0.02 md. In GB-1, about 50% of the gas came from a single fracture between 4000 and 4020 ft deep, and most of the remainder came from bedding planes in the Fruitland zone, between 3800 and 3882 ft. In GB-2, most of the gas came from a fracture near the top of the Pictured Cliffs. In view of the complex flow pattern, values of reservoir characteristics derived from flow tests must be considered apparent only.

We expect the 26-kt nuclear explosion at the base of the Pictured Cliffs to create a chimney between 330 and 400 ft high with a radius of 78 ft. Fracturing should extend radially about 400 ft. No flooding of the chimney with water is expected. The chimney gas is expected to contain about 200 μC of tritium and 2 μC of Kr^{85} per cubic foot of gas at normal temperatures and pressures. Rapid flaring of three chimney volumes might reduce these concentrations by a factor of ten.

INTRODUCTION

This is a report on the status of the Gasbuggy experiment as of September 20, 1967. Gasbuggy will be a nominally 26-kt detonation at a depth of 4240 feet; its purpose is to determine to what extent an underground nuclear explosion can stimulate the production of natural gas from low-permeability formations. Almost all the preshot field work has been completed, and most of the data have been reduced though not all have been analyzed. Detailed plans for programs at the time of the shot are essentially complete, and hardware for the dynamic measurement instrumentation and the device-emplacement system has been manufactured.

The objectives of the Gasbuggy experiment are:

1. To measure the changes in the deliverability and ultimate recovery of the gas and to identify the mechanisms responsible for these changes;

2. To measure the radioactive contamination of the gas, to study the thermodynamics of the mixture of methane and gaseous fission products, and to use this information in evaluating possible control measures; and

3. To measure and evaluate the generation of seismic energy and its propagation within the San Juan Basin, as part of a continuing study of ground motion and its effect on structures.

The preshot phases of the technical program established base lines, the conditions with which the results of the shot can be compared. Thus, the field program involved measurement of the gas-flow properties from the area of the experiment, a detailed geologic and geophysical exploration program, and a hydrologic test and evaluation program. Laboratory work included measurements of physical properties of the rock most strongly affected by the explosion, computation of dynamic shock effects, assessment of the expected gas quality, transient gas-flow computations, and evaluations of ground shock and other hazards.

PARTICIPANTS

Gasbuggy is sponsored jointly by the U.S. Government and the El Paso Natural Gas Company (EPNG). The overall technical responsibility for the execution of the Gasbuggy experiment rests with the Lawrence Radiation Laboratory (LRL), which is operated by the University of California for the Atomic Energy Commission. W. Woodruff, LRL, is responsible for the execution of the technical program. Technical personnel from the U.S. Bureau of Mines, EPNG, and LRL cooperated in the design and execution of many of the preshot programs, under the direction of F. Holzer (LRL) and C. Atkinson (BuMines). L. Truby (EPNG) contributed materially to the drilling and exploration program. Gas-flow measurements were specified and interpreted by C. Atkinson and D. Ward (BuMines) and R. Lemon (EPNG); H. Kendrick (EPNG) was responsible for the measuring equipment at the site. Geological and geophysical data were analyzed and interpreted by M. Spitler (EPNG), D. Rawson (LRL), R. Pritchard (EPNG), and J. Fassett, U.S. Geologic Survey (USGS). Hydrologic tests and evaluations were by J. Korver (LRL) and F. Koopman (USGS). C. Sisemore and D. Power (LRL), W. Perret (Sandia Laboratory), and R. F. Beers (Environmental Research Corporation) are in charge of dynamic measurement programs.

THE GASBUGGY SITE

The Gasbuggy site is near the eastern edge of the San Juan Basin, about 70 road miles from Farmington, New Mexico, in the southwest quarter of Section 36, Township 29N R4W of Rio Arriba County. The area is within the Carson National Forest and is covered by oil and gas leases owned by EPNG. A map of the area is shown in Fig. 1. The locations of a number of EPNG wells are indicated on the map; Table I summarizes the production history of these wells. Production from this area is extremely low, and the anticipated ultimate recovery varies widely from well to well, depending on the degree of natural fractures encountered.

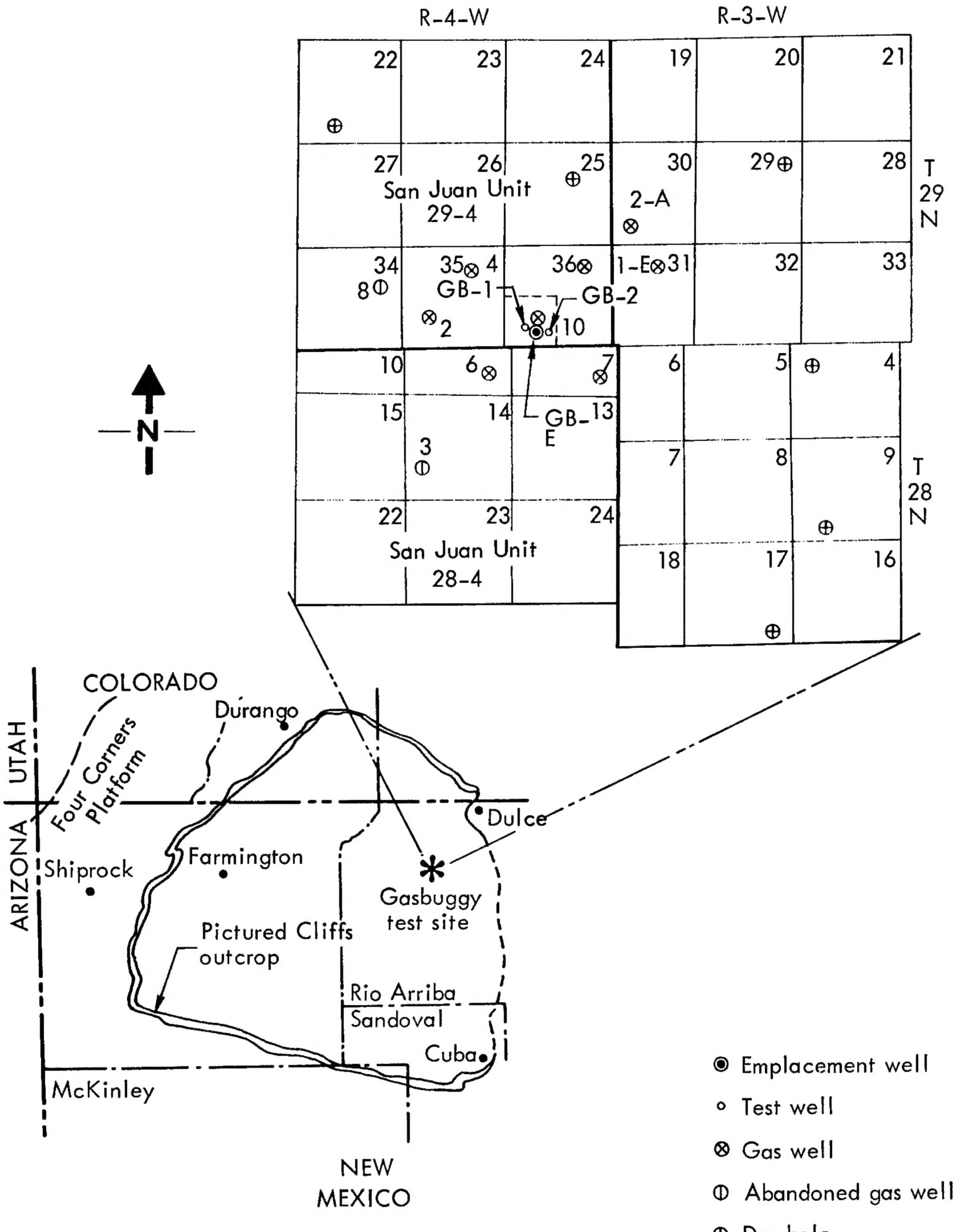

Fig. 1. Gasbuggy test-site area.

Table I. Choza Mesa–Pictured Cliffs field production history.

	Well							
	28-4 No. 6	28-4 No. 7	29-4 No. 2	29-4 No. 4	29-4 No. 10	29-4 No. 16	Indian A-2	Indian E-1
Location (section-township-range)	11-28-4	12-28-4	35-29-4	35-29-4	36-29-4	36-29-4	30-29-3	31-29-3
Initial potential (Mcf/day)	3182	1058	6928	801	1348	635	5709	20,200
AOF (Mcf/Day)	–	–	–	–	1403	647	7984	–
Annual production (M^2cf)								
Year								
1955	1.7	4.3	–	–	–	–	–	138.8
1956	11.0	–	144.6	9.2	–	–	–	37.2
1957	–	–	89.3	4.1	2.3	–	–	–
1958	18.6	6.1	84.2	2.6	12.5	–	131.7	63.4
1959	12.1	5.0	60.2	6.0	9.0	5.7	108.9	23.8
1960	12.4	4.3	42.7	4.5	8.2	3.9	68.6	23.3
1961	11.9	4.8	44.9	4.4	8.5	4.3	53.8	8.7
1962	10.3	3.1	39.5	2.9	9.3	3.1	47.7	10.5
1963	10.6	3.9	39.0	2.2	7.5	3.6	32.7	11.7
1964	10.0	4.1	24.2	2.4	6.6	4.2	17.1	5.7
1965	8.1	4.8	33.0	1.7	8.6	3.7	26.3	8.8
1966	5.8	4.1	30.1	2.3	8.4	2.9	34.6	6.7
Cumulative Production, Jan. 1, 1967 (M^2cf)	112.5	44.5	631.7	42.3	80.9	31.4	521.4	338.6
1966 New Mexico State test (Mcf/Day)	20	14	112	8	22	4	129[a]	27

[a] 1965 test

STRATIGRAPHY

The formation selected for the nuclear-stimulation experiment is the Pictured Cliffs sandstone, which is about 285 ft thick at the Gasbuggy site and whose base is about 4200 ft below the surface. The position of this formation within the basin structure is shown in Fig. 2. At the Gasbuggy site the structure of the Pictured Cliffs takes the form of a bench, as shown by the isopach map of Fig. 3.

Two exploratory holes, GB-1 and GB-2, were drilled to determine the subsurface environment in the immediate neighborhood of the detonation location. Neither hole was artificially stimulated. Figure 4 shows the location of these holes in plan view and the stratigraphic column they revealed. In general, the stratigraphies differed little between the two holes. From the surface to a depth of about 3480 ft, the rock consists of the alternating sandstones and shales of the San Jose and Nacimiento formations. The boundary between these two formations is at about 1870 ft, as evidenced by an apparent break in the velocity and density logs. Immediately below is the Ojo Alamo sandstone, extending to about 3650 ft. Between the Ojo Alamo and the top of the Pictured Cliffs sandstone are the shales and coals of the Kirtland and Fruitland formations. The Kirtland shale extends from 3650 to 3800 ft below the surface, then gradationally changes into the Fruitland formation. Interbedded coals and shales make up the first 80 ft of the Fruitland stratum; the part between 3880 and 3915 ft is mostly coal. The Pictured Cliffs sandstone, starting at a depth of 3915 ft and extending to about 4200 ft, can be divided into three parts. The upper part, from 3916 to 4046 ft, is a massive sandstone interbedded with thin beds of shale. The so-called Fruitland tongue, between 4046 and 4066 ft, is a sequence of shale, coal, and siltstone. From 4066 to 4200 ft the lower Pictured Cliffs is again a massive sandstone with a few thin beds of shale. Below 4200 ft this sequence blends into the siltstones and shales of the Lewis formation.

ROCK PROPERTIES

The entire Pictured Cliffs formation was cored in GB-1, and all but a few feet was cored in GB-2. A total of 547 ft of core was taken from the two holes. Samples were taken from the core at 2-ft intervals,

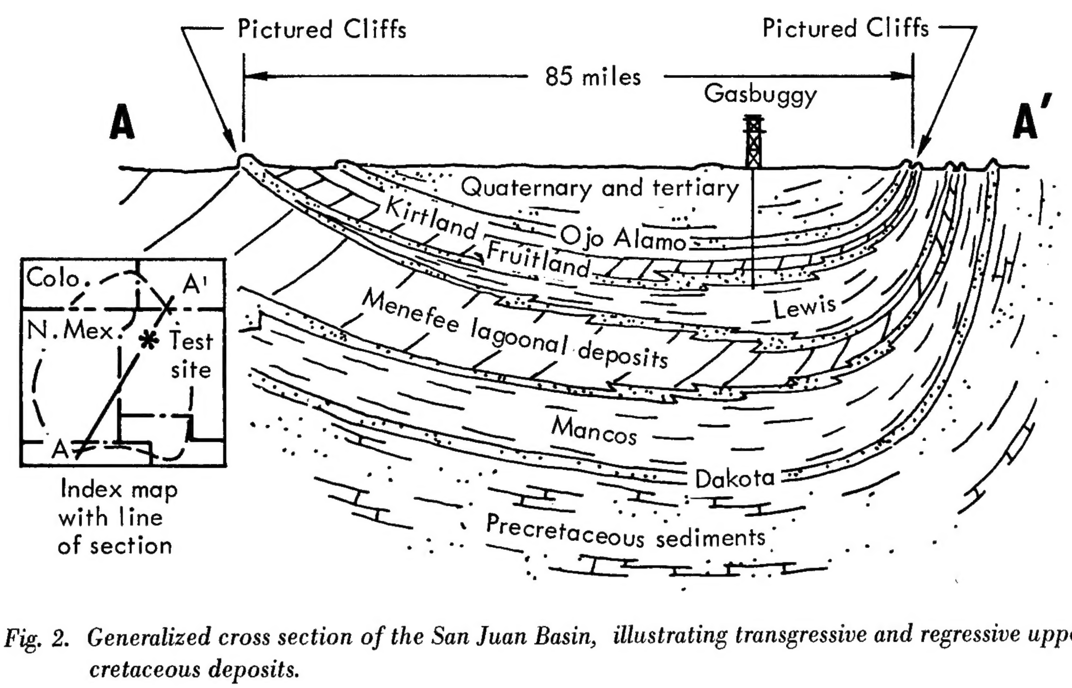

Fig. 2. Generalized cross section of the San Juan Basin, illustrating transgressive and regressive upper cretaceous deposits.

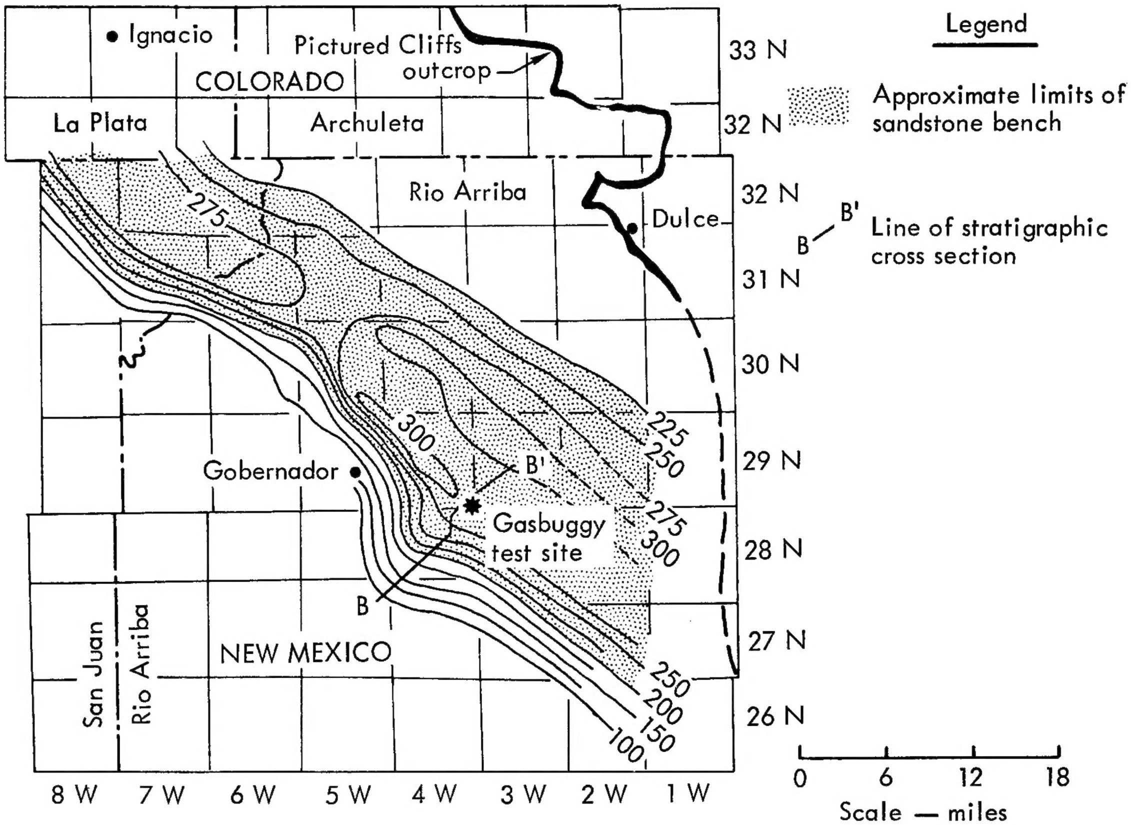

Fig. 3. Gross isopach map of Pictured Cliffs sandstone.

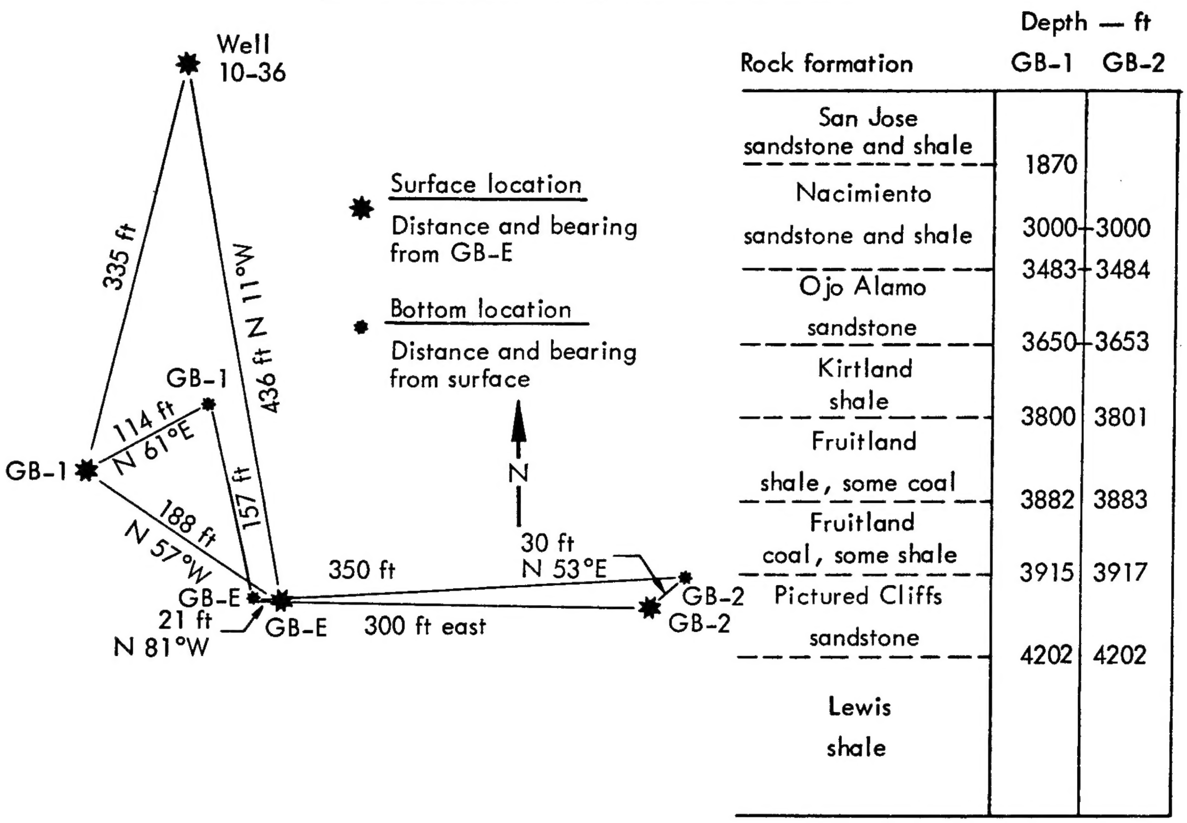

Fig. 4. Hole-location plan and stratigraphic column.

preserved in foil and wax to minimize water loss, and analyzed for porosity, permeability, oil saturation, and water saturation by Core Labs, Inc. Selected samples were analyzed for mineralogical content and elemental composition and subjected to petrographic examination. Other samples were tested for bulk density, compressional and shear velocity, compressibility, and various strength characteristics. Data are summarized in Tables II and III and Fig. 5. Little difference was found in the properties of samples from GB-1 and GB-2, and, in general, the results obtained by different measurement techniques agree quite well. The velocity logs indicated higher velocities in the Pictured Cliffs than did the core measurements; this difference may be an overburden effect.

Fractures and Permeability

Information on fractures was obtained from core examination, borehole photography, and the Birdwell focus 3-D sonic log, and corroborated by temperature logs and packer flow-meter production logs. This information, together with the porosity and permeability as established by core analysis, is shown in Fig. 5. A vertical fracture encountered between 4000 and 4020 ft in GB-1 corresponds to a major gas entry. Similarly, most of gas production in GB-2 occurred at the top of the Pictured Cliffs, where two vertical fractures were encountered during coring. Since these fractures in GB-2 were later filled with cement so that coring could proceed, the gas-production log of the remainder of the hole does not include this entry. Initially, however, three times more gas was produced from these fractures than from the remainder of the hole. Aside from these cited instances, there is no close correlation between gas entries and fracture locations, zones of high porosity, or regions of relatively high permeability. The permeability data in Fig. 5 are from core analyses and range from a little less than 0.01 to a few tenths of a millidarcy, with an average of approximately 0.16 md. However, analyses of pressure-buildup data (discussed below) indicate an in-situ permeability in the neighborhood of 0.01 to 0.02 md. This difference may be attributable to the lithostatic overburden pressure to which the in-situ material is subjected. Further investigation is necessary before any definite conclusion can be reached.

Composition of Reservoir Rocks and Fluids

The chemical constituents of the various rock formations and of the water and gas produced at the Gasbuggy site are being determined. One purpose of this analysis is to establish the composition of the rock in the immediate vicinity of the detonation point so that the formation of radioactive activation products can be calculated. The water and gas found in various strata are being analyzed to aid in identifying the origin of the fluids that will be obtained in the post-shot exploration and sampling program. Thus, if water is encountered near the bottom of the chimney in the close-in hole, its chemical analysis will help to establish whether it came from the Fruitland or Lewis formations or migrated from the Ojo Alamo. Available analyses are shown in Tables IV, V, and VI.

HYDROLOGY

During the early design stages of the Gasbuggy technical program, we recognized the need to establish hydrologic properties of aquifers that might communicate with the chimney after the explosion. From previous drilling experience near the Gasbuggy site, the Ojo Alamo and Fruitland formations were identified as possible aquifers. However, since no water was encountered in the Fruitland in either GB-1 or GB-2, the hydrology tests were confined to the Ojo Alamo.

In GB-1 the Ojo Alamo was tested in two parts. The core drilling was stopped at a shale break at about 3578 ft, and the interval between 3481 and 3578 ft was packed off and subjected to several swab and recovery tests. Coring then continued to 3696 ft, and the interval between 3578 and 3696 ft was similarly packed off and tested. Although the contact between the Ojo Alamo and the Kirtland is at about 3654 ft, the Kirtland is devoid of water, so that the inclusion of its upper part in the hydrologic testing does not affect the results. In GB-2 the Ojo

Table II. Summary of density, velocity, porosity, and water content.

Rock Formation	Depth (ft) GB-1	Depth (ft) GB-2	Average grain density (g/cc) GB-1 CL	Average bulk density (g/cc) GB-1 Schl	Average bulk density (g/cc) GB-1 CL	Average bulk density (g/cc) GB-2 Schl	Average bulk density (g/cc) GB-2 CL	Compressional velocity (ft/sec) GB-1 Schl	Compressional velocity (ft/sec) GB-2 Schl	Compressional velocity (ft/sec) GB-2 Bw	Shear-wave velocity (ft/sec) GB-2 Bw	Total porosity (% by volume) GB-1 Calculated[d]	Total porosity (% by volume) GB-1 CL[e]	Total porosity (% by volume) GB-2 CL[e]	Water content (% by weight) (Core Lab data) Free GB-1	Free GB-2	Bound GB-1	Bound GB-2	Total GB-1	Total GB-2
San Jose sandstone and shale	500–1870			2.207				10,790												
Nacimiento sandstone and shale	1870–3000–3483	2400–3000–3484		2.382; 2.45		2.417		12,590; 13,090		13,670	7,830									
Ojo Alamo sandstone	3483–3650	3484–3653	(3)[a] 2.65	2.432	(53) 2.38	2.472		14,170		15,700	9,250	(53) 10.6	(53) 10.3	9.1[f]	(53) 3.32		(53) 3.83		(53) 7.28	
Kirtland shale	3650–3743–3800	3653–3801	(3) 2.68	2.472[b]	(7) 2.56	2.537		13,160		14,070	7,480									
Fruitland shale, some coal	3800–3882	3801–3883		2.29[b]	(19) 2.53[c]	2.357				11,700	6,780									
Fruitland coal, some shale	3882–3915	3883–3917		1.646		1.695				8,850	5,480									
Pictured Cliffs sandstone	3915–4202	3917–4202	(6) 2.69	2.468	(141) 2.465	2.507	(110) 2.468		13,520			(141) 9.3	(141) 9.0	(110) 10.4	(141) 2.02	(110) 2.85	(141) 2.90	(110) 1.23	(141) 4.92	(110) 4.08
Lewis shale	4202–4228–4318	4202–4244–4270	(3) 2.71	2.583	(8) 2.606	2.587	(5) 2.58		13,700			(8) 5.9	(8) 5.0	5.9	(8) 1.59	(5) 1.80	(8) 2.19	(5) 1.66	(8) 3.78[c]	(5) 3.46

CL: Core Lab; Schl: Schlumberger; Bw: Birdwell

[a] (3), etc., is the number of samples tested.

[b] Poor borehole conditions; data questionable.

[c] Samples not representative of the average—mostly very fine-grained sandstone.

[d] Calculated from Core Lab free-water and grain-density data and bulk density from Schlumberger

[e] Porosity available to fluids.

[f] Birdwell geophysical log interpretation.

Table III. Some properties of samples selected as typical for detailed chemical and physical characteristics.

Rock formation	Sample No.	Depth (ft)	Bulk density (g/cc)	Free water (% by weight)	Compressional velocity (ft/sec)	Shear velocity (ft/sec)
	L-18[a,b]	4267	2.621	–	13,165	9,100
	L-18[c]	4267	2.622	–	14,300	9,300
Lewis	L-13	4280	2.612	1.9	–	–
	L-12[d]	4281	2.62	–	13,120	8,040
	L-8[a]	4294	2.639	–	12,250	8,580
	P-47	3946	2.48	2.7	–	–
	P-39	3991	2.46	–	–	–
Pictured Cliffs	P-27[a]	4073	2.528	–	11,200	8,100
	P-24	4094	2.48	2.7	–	–
	P-22[d]	4101	2.44	–	8,200	7,120
	F-4[a]	4188	2.357	–	10,670	7,170
Fruitland	F-5	3880	2.492	4.3	–	–
	F-3	3886	1.709	2.1	–	–
Kirtland	K-9	3690	2.58	2.6	–	–
Ojo Alamo	0-10	3494	2.428	4.2	–	–

[a]Measurements by P. Knauss (LRL); other measurements by D. Stephens (LRL).

[b]Parallel to bedding.

[c]Perpendicular to bedding.

[d]Data from C. Sisemore (LRL).

Table IV. Composition of a composite sample of the Lewis shale.

Component	% by weight
Silica	64.0
Ferric oxide	4.4
Aluminum oxide	10.1
Calcium oxide	4.2
Magnesium oxide	2.4
Titanium oxide	1.1
Manganese oxide	0.05
Potassium oxide	2.3
Sodium oxide	2.1
Phosphorus pentoxide	0.3
Sulfur	0.58
Carbon dioxide	4.6
Carbon (free or H_xC_x)	0.18
Water (total)	3.6

Table V. Representative gas analysis, GB-1.

Component	Mol. %
Methane	85.36
Ethane	7.40
Propane	4.00
1-Butane	0.75
N-Butane	0.94
1-Pentane	0.29
N-Pentane	0.20
Hexane	0.18
Nitrogen	0.59
Carbon dioxide	0.29
Helium	Trace
Heating value (Btu/ft^3)	1178
Specific gravity	0.673

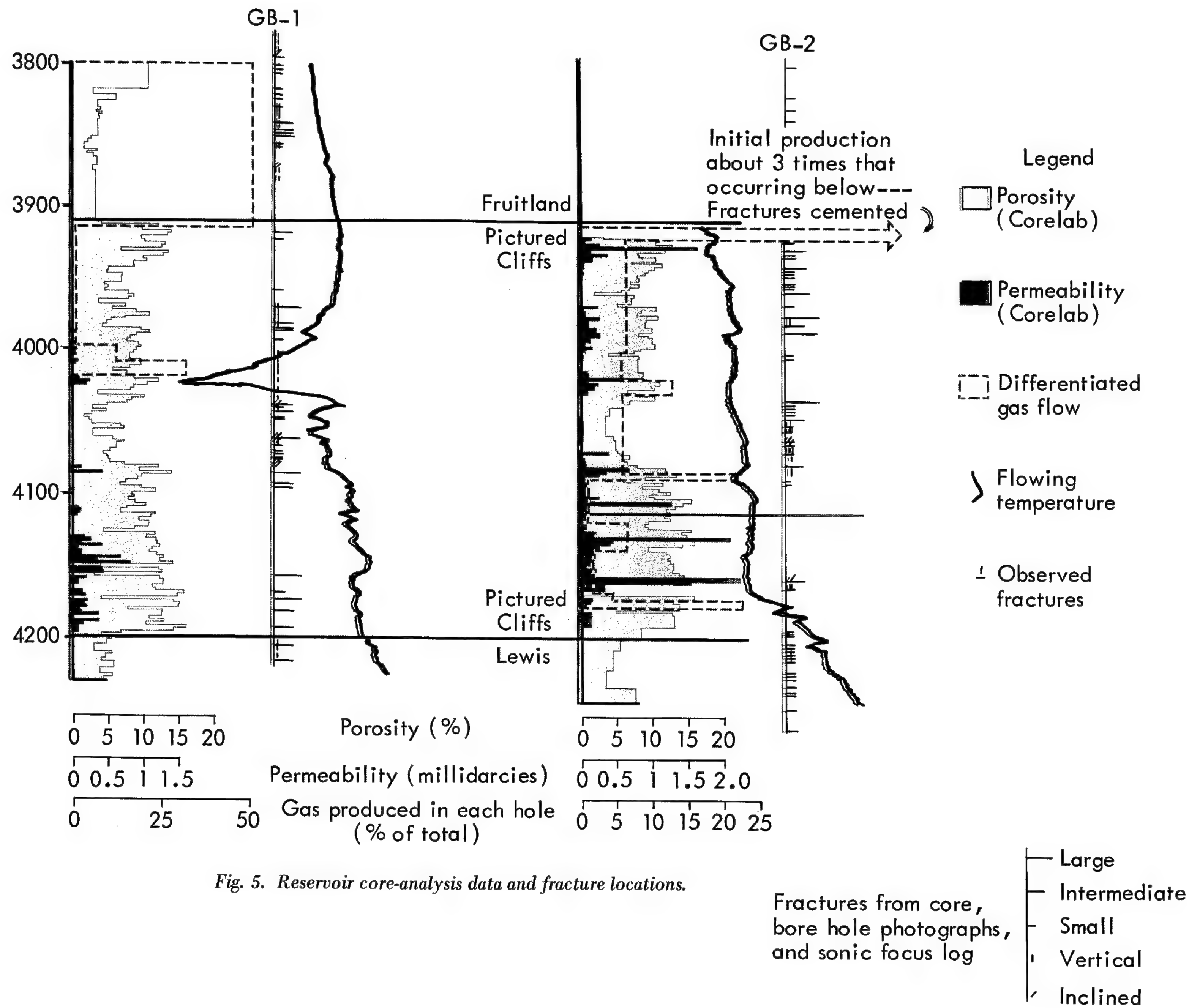

Fig. 5. Reservoir core-analysis data and fracture locations.

Table VI. Water analysis.

	Well No. 10-36 Pictured Cliffs formation	Hole GB-1 Ojo Alamo formation
Constituents, (ppm)		
Sodium	713	2400
Calcium	31	340
Magnesium	11	15
Chloride	2673	170
Iodide	9	–
Bicarbonate	1577	195
Sulfate	–	5470
Total solids	5014	8900
Specific gravity at 60°F	1.006	1.014
pH	6.1	9.5

Alamo was tested as a single unit in the interval between 3478 and 3654 ft. Only one swab test and one recovery test were performed.

Results of these tests are shown in Table VII. In calculating the hydrostatic head from the recovery curves, it was assumed that the upper and lower sections of the Ojo Alamo are connected and have the same hydrostatic head. The permeability-thickness (kh) products were computed from the swabbing tests by a modified Skibitzke equation for bailer tests. By examining the core from GB-1 and the density logs from both GB-1 and GB-2, it was concluded that about 146 of the total 173 ft is water producing.

These data were next used to assess the amount of water that might be introduced into the chimney if the chimney or fractures extending from it should intersect the Ojo Alamo. The calculations were made with a two-dimensional, non-steady-state computer code. The first case assumed that a chimney of infinite permeability, 150 ft in diameter, intersected the entire Ojo Alamo; the second case assumed that a linear fracture, as wide as the chimney, extended through the entire Ojo Alamo. In both cases it was assumed that the chimney pressure did not change and that the aquifer acted as a homogeneous isotropic system of infinite extent. Effects of gravity were neglected. Results of the calculation are shown in Fig. 6 for two pressures: 1000 psi, corresponding to the approximate formation pressure, and 800 psi, corresponding to an assumed back pressure during reservoir testing after the shot. The water level in the chimney corresponding to these volumes depends on the assumed chimney porosity. A porosity ranging from 15 to 25% is considered likely. With this porosity range and with a shot point 40 ft below the Pictured Cliffs-Lewis shale contact, the water level will probably not rise into the Pictured Cliffs during the first year and a half after the shot.

Table VII. Hydrologic properties of the Ojo Alamo.

	GB-1	GB-2
Static water level (ft below surface)	927	883
Permeability-thickness, kh (md-ft)		
3481 to 3578 ft	48.17	–
3578 to 3654 ft	106.29	–
Average, 3481 to 3654 ft	71.02	76.53

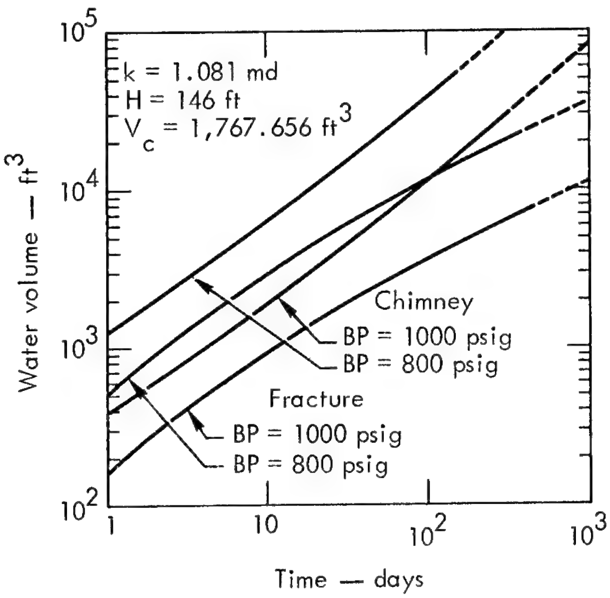

Fig. 6. Gasbuggy water influx from Ojo Alamo.

GAS–FLOW TESTS AND RESERVOIR ANALYSIS

The Gasbuggy reservoir evaluation has been primarily based on (1) an analysis of the core and logs of the naturally completed, gas-drilled holes GB-1 and

GB-2 for the amount of gas in place; (2) a characterization of the gas entries into GB-1 and GB-2 by means of flowing temperature logs, packer flow meters, and natural gages; and (3) a series of drawdown and buildup tests to determine permeability thicknesses and flow characteristics.

An analysis of the data in Fig. 5 shows that the total gas-in-place represented by the total gas-saturated section is about 5.8 bcf per 160 acres. Considering only the sections where the water saturation is 60% or less, this value becomes 4.7 bcf. The relevant data for both GB-1 and GB-2 are summarized in Table VIII.

While not all fractures identified in the core appeared to produce gas during the testing for entries, the flow of gas into holes GB-1 and GB-2 seems primarily associated with the occurrence of natural fractures. This is also borne out by Fig. 7, which shows the record of natural flow gages taken during the core drilling of GB-1, and by Fig. 8, which presents the packer flow-meter data. These tests showed that about 50% of the gas in GB-1 came from the Fruitland. Since this formation shows no measurable porosity, the flow must come from weaknesses connecting with the Pictured Cliffs gas. Similar data are not available from GB-2, since the casing in this hole was set to the top of the Pictured Cliffs. However, a large gas entry was found at about 3920 ft in GB-2 when drilling commenced below the casing point. The fracture responsible for this gas flow had to be cemented to keep the hole dry, and its contribution is therefore not shown in Fig. 8. It is estimated that this fracture produced at least three times more gas than the rest of the hole. Production from below 3920 ft was generally less than 10 Mcf/day. The data from the packer flow-meter log show that even this very low gas flow is primarily supported by fractures, weaknesses, or bedding planes, rather than by uniform production from the matrix. That the Gasbuggy reservoir is strongly influenced by fracture distribution is also borne out by the history of the other wells in the area, as shown in Table I. Six of the wells average less than 27 Mcf/day. High initial natural flow rates in three wells indicate that natural fractures had been encountered.

The schedule of flow tests conducted on GB-1 is given in Table IX. Pressure buildup curves from GB-1 are shown in Fig. 9. Curve 1 represents the pressure buildup in GB-1 upon completion of the hole; Curve 2, the buildup following the fourth flow-rate run of the first series of isochronal tests; Curve 3, the buildup following the 30-day flow test; and Curve 4, the buildup after the constant-flow-rate test at the sand face. These data indicate a reservoir pressure of approximately 1050 psia, as compared with an original pressure of approximately 1259 psia for the area. The calculated permeability-thickness (kh) products derived from these curves range from 1.7 to 3.0 md-ft. The nature of the gas entries through the fracture network makes the identification of a producing thickness questionable; however, on the basis of an examination of the core, a thickness of about 150 ft was assigned to such an interval. This yields permeabilities of between 0.01 and 0.02 md.

Figure 10 shows the pressure drawdown versus time recorded during the 30-day flow test. The slope changes significantly at about 16 days. The kh

Table VIII. Reservoir properties.

	Gas-saturated sand with 60% or less water saturation			Total gas-saturated sand		
	GB-1	GB-2	Average	GB-1	GB-2	Average
Porosity (%)	11.2	12.4	11.8	9.6	10.6	10.1
Gas saturation (%)	52.0	52.7	52.3	42.5	41.8	42.1
Permeability (md)	0.14	0.19	0.16	0.10	0.15	0.12
Thickness (ft)	156	149	152.5	254	255	254.5
Temperature (°F)	130	130	130	130	130	130
Pressure (psia)	1050	–	–	1050	–	–
Gas-in-place[a] (bcf/160 acres)	4.512	4.912	4.712	5.504	6.064	5.784

[a]Gas volumes expressed at 15.025 psia and 60°F.

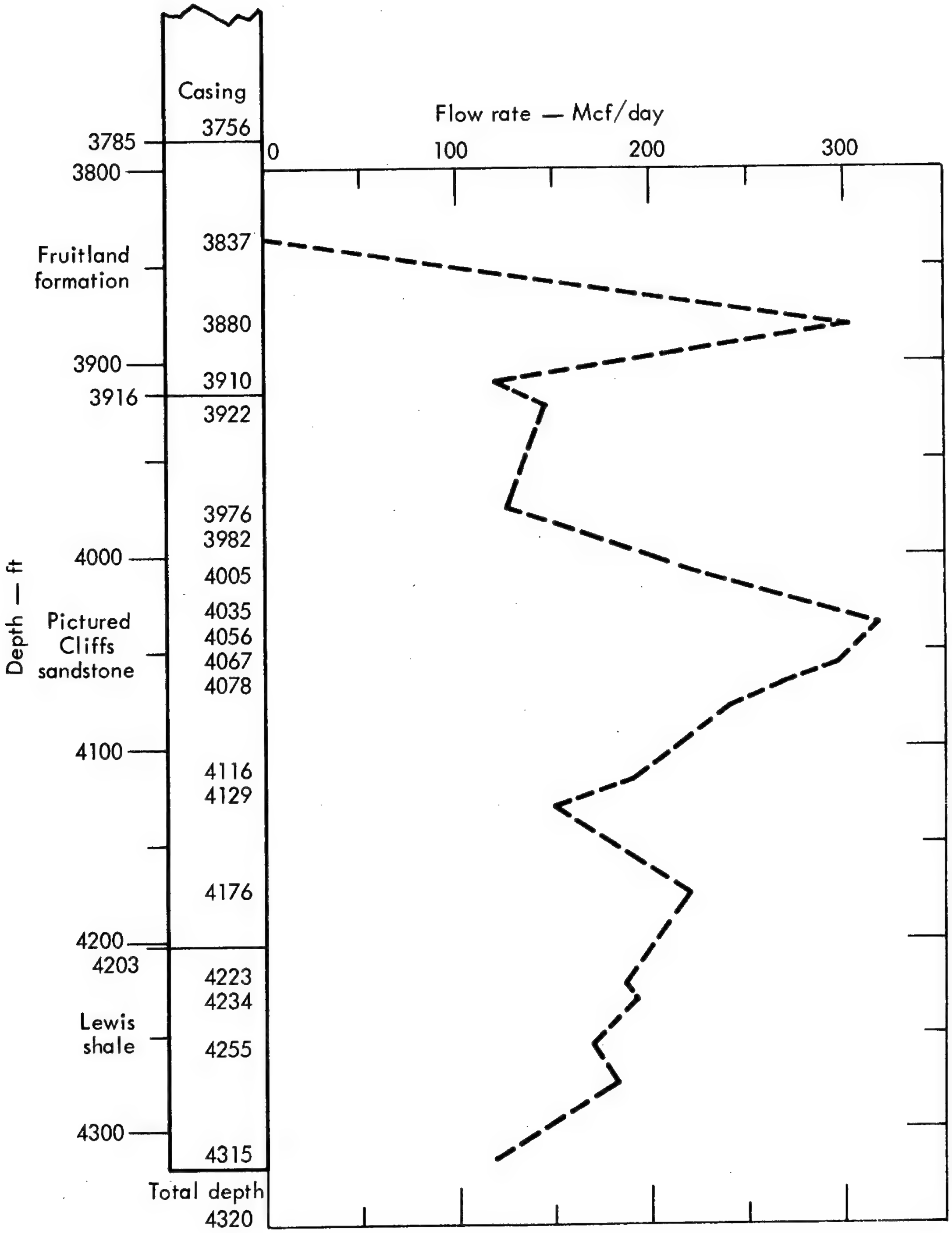

Fig. 7. Natural gas flow rates while core drilling, GB-1.

values indicated by the two portions of this curve are 3.4 and 1.0 md-ft, respectively. Figure 11 shows the result of one of the isochronal test series. The slope of the back-pressure curve is 0.735.

In general, the flow rates from GB-1 and GB-2 are characteristic of low-permeability reservoirs. Thus, after completion of the standard 3-hr New Mexico State potential test, GB-1 was allowed to flow for

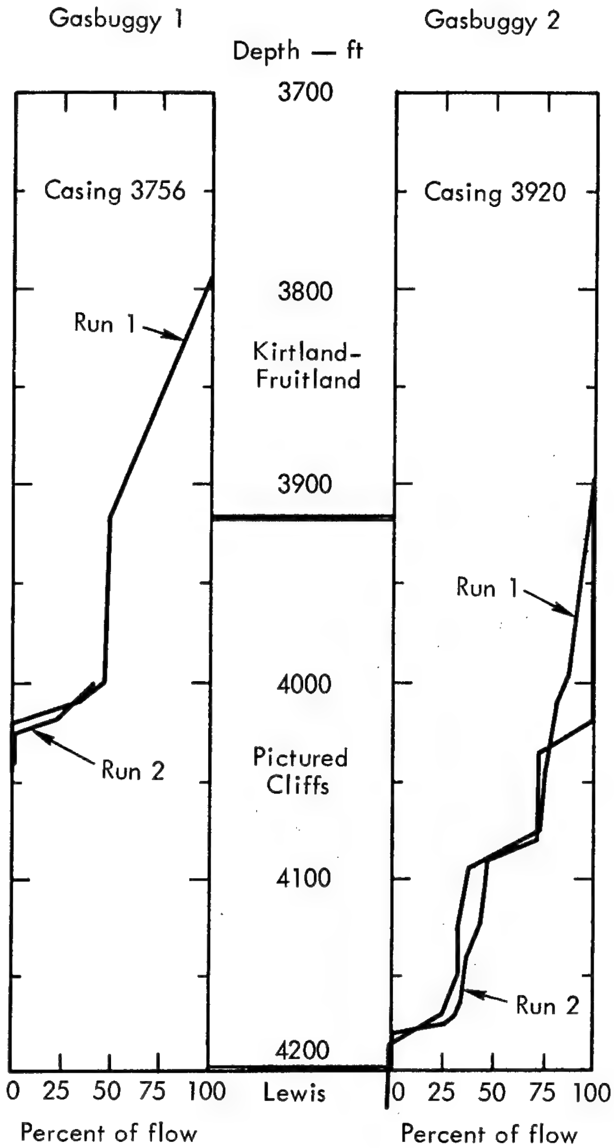

Fig. 8. Integral packer flowmeter logs.

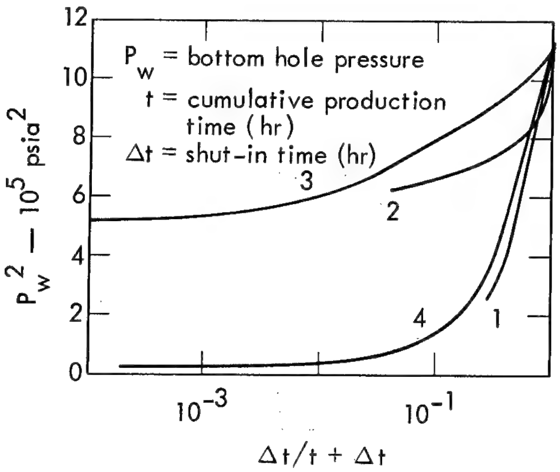

Fig. 9. Pressure buildup, GB-1.

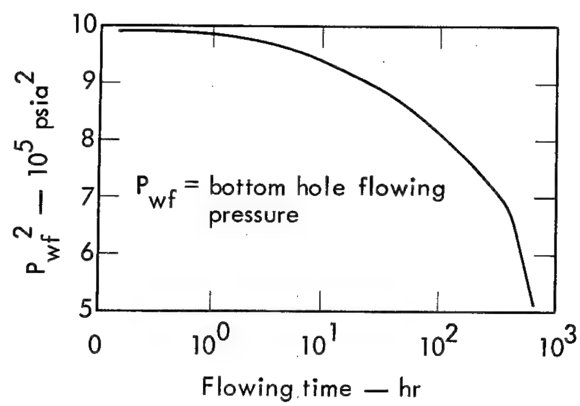

Fig. 10. Pressure drawdown, GB-1

several days. After 4.7 days the flow rate was 35 Mcf/day. Two flow tests were performed on GB-2; the average rate of flow was 5.5 Mcf/day in the first test and 4.5 Mcf/day in the second.

Natural or induced fractures have created a complex flow pattern in the reservoir; because of this complexity, reservoir characteristics derived from the various drawdown and buildup tests must be considered as apparent values only.

Table IX. Schedule of flow tests, GB-1.

Test Event	Flow data Rate (Mcf/day)	Duration (hr)	Shut-in pressure data Duration (hr)	Observed BHP (psia)
Shut-in after penetration Pictured Cliffs formation			18	560
Shut-in following completion of coring operations			164	910
First series of isochronal flow tests				
1st flow rate	274	6		
pressure buildup			27	905
2nd flow rate	90	6		
pressure buildup			11	911
3rd flow rate	440	6		
pressure buildup			47	912
4th flow rate	146	24		
pressure buildup			934	1009
Second series of isochronal flow tests				
1st flow rate	415	6		
pressure buildup			68	1000
2nd flow rate	264	6		
pressure buildup			70	1000
3rd flow rate	148	6		
pressure buildup			49	1000
4th flow rate	75	720		
pressure buildup			878	995
Constant withdrawal at the sand face, surface flow rate	600-108	112		
Pressure buildup			478	954
New Mexico State Potential Test, flow rate at the end of 3 hr	447			

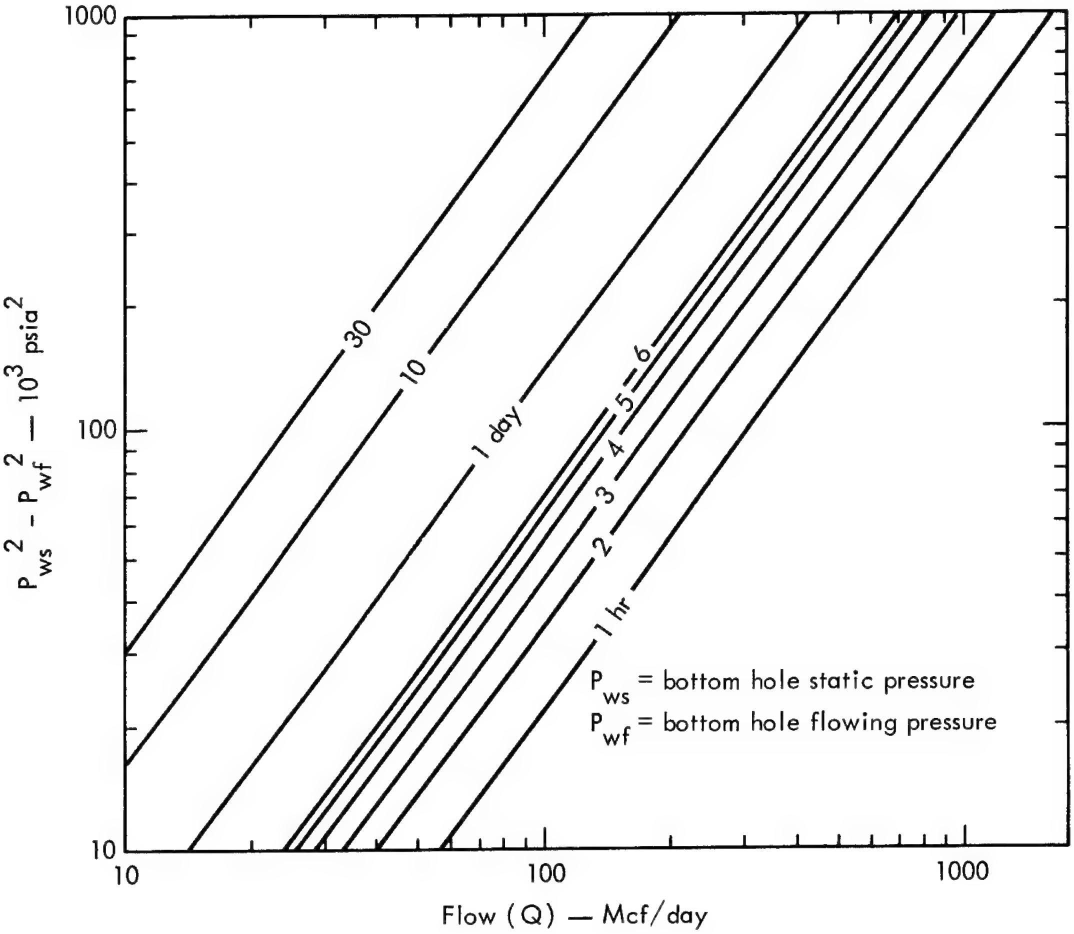

Fig. 11. Isochronal performance curve, GB-1.

EXPECTED EFFECTS

A number of the dynamic effects expected from the explosion have been studied. Among them are the formation of the cavity and the subsequent growth of the chimney, the extent of both radial and vertical fractures, ground motion as a function of distance, and the expected concentration of radionuclides in the gas to be withdrawn from the chimney.

The final radius of the spherical cavity and the extent of material failure from the detonation center were predicted by a numerical technique that describes material response to a propagating stress field. This calculation makes use of the relevant equations of motion and depends on the proper equation of state of the material and on a unique description of its failure. For Gasbuggy, samples from the Lewis shale, the Pictured Cliffs sandstone, and the Fruitland coal were measured for static and dynamic compressibilities and failure characteristics. Assuming a yield of about 26 kt, calculations predict a cavity radius of 78 ft and laterial cracking in the Pictured Cliffs formation to 393 ft from the explosive. The same calculations show that the Fruitland coal tongue 334 ft above the explosion center may stop the cracks. The calculations cannot predict actual chimney height. Comparisons with past events show chimney heights to be within about 15% of calculated fracture limits. If the Fruitland coal can prevent the collapse of the over-burden material, then the Gasbuggy chimney may not extend above 330 ft from the energy source. Otherwise it could extend into the Fruitland.

Another study concerns the expected concentrations of radioactive gases from the Gasbuggy chimney. Preparations have been made to sample and analyze this gas. Calculations of expected concentrations have also been used to guide the post-shot sampling and drilling program and to prepare for any possible hazards in withdrawing from the chimney. In addition, a series of computations was performed to evaluate how the rapid flaring of chimney gas and its replacement by formation gas might affect the concentrations of various radionuclides. The results suggest that rapid flaring could substantially decrease radionuclide concentrations in any gas produced afterwards.

While several radionuclides have been considered, major emphasis was placed on I^{131}, Kr^{85}, and tritium, which are the ones most likely to cause problems. For the expected concentrations of I^{131} and Kr^{85}, it was assumed that all of these volatile species produced will end up in the chimney gas. For tritium, the equilibrium distribution of hydrogen between water and the permanent gases expected in the cavity was determined from a thermodynamic calculation. This distribution, as well as the ratio of H_2 to CH_4, was computed for 1700°C, where about 30% of the hydrogen is in the form of water. The results for I^{131}, Kr^{85}, and tritium (in the forms of HT and CH_3T) are shown in Figure 12. The amount of tritium in the form of HTO is not included in this figure, since it would not be in the gas phase and hence could be easily removed from the product stream. I^{131}, with its 8-day half-life, decays rapidly, while both Kr^{85} and tritium, whose half-lives are 10.6 and 12.6 years, respectively, show no such decay. Figure 12 also shows the decrease in concentration that is expected to follow the rapid flaring of three chimney volumes of gas.

The concentrations of tritium and Kr^{85} in the combustion products after burning of the gas were also considered. Burners generally dilute each volume of gas by about 200 volumes of air to keep CO and CO_2 to permissible levels, and a similar reduction (ignoring any pipe-line dilution) would take place in any radionuclides in the gas.

Other studies have yielded expected values of ground motion from the Gasbuggy explosion. These studies were made not only from the consideration of public safety but also as a guide for setting up the surface seismic instrumentation. Ground-motion predictions were based on extensive data from underground detonations at the Nevada Test Site in environments similar to the sandstones and shales at Gasbuggy. In general, surface motion on soil or

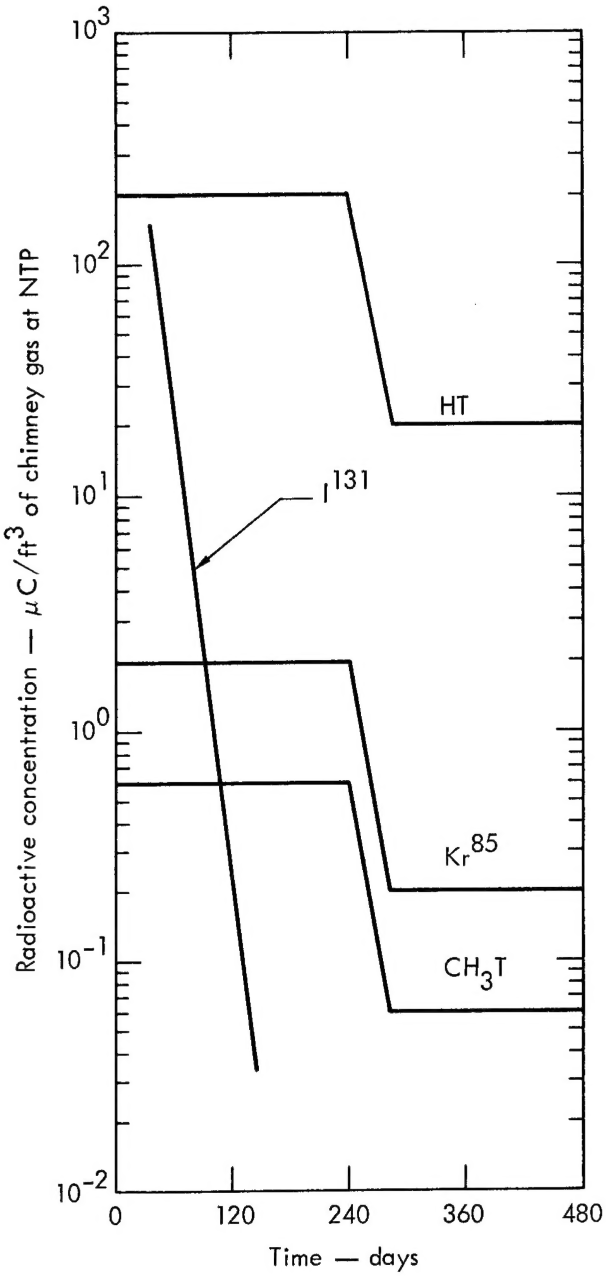

Fig. 12. Expected concentrations of Kr^{85}, I^{131}, and T in chimney gas.

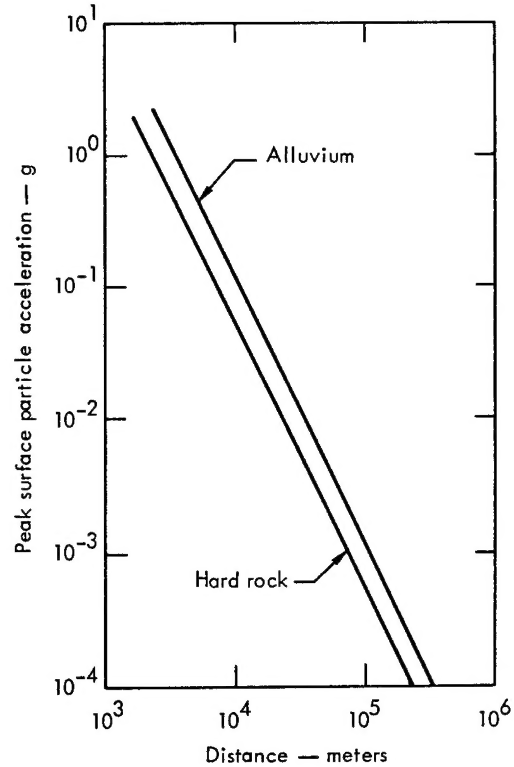

Fig. 13. Predicted peak surface particle acceleration versus slant distance in alluvium and hard rock.

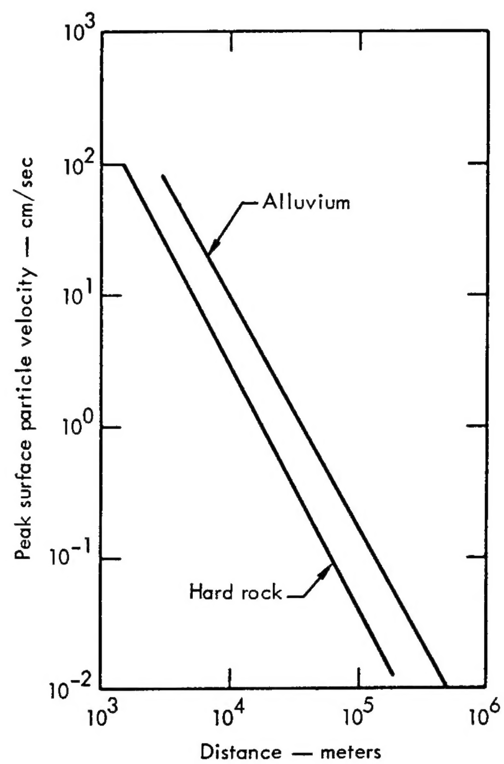

Fig. 14. Predicted peak surface particle velocity versus slant distance in alluvium and hard rock.

poorly consolidated materials will be greater than on hard rock. Expected accelerations and velocities as functions of distance are shown in Figures 13 and 14. These curves were derived from data which show considerable scatter. In general, one standard deviation corresponds to a departure from these curves of a factor of 2.

SHOT-TIME MEASUREMENTS

The measurement program during and immediately following the Gasbuggy explosion will concern itself with subsurface measurements of the outgoing shock wave, surface motion measurements, and a number of safety-related measurements such as precautionary monitoring for radioactivity. The subsurface and surface measurements are being made to establish the validity of the predictive calculations and to aid in the interpretation of the results. Shock instrumentation will be installed in holes GB-1, GB-D, and GB-E. Measurements in GB-1 and GB-E are primarily designed to study the outgoing shock wave, the generation of fractures, and the collapse of the chimney. Quantities to be measured include peak shock pressure, times of shock arrivals, fracture radii, and the history of chimney collapse. GB-D will be instrumented with acceleration and velocity gages, primarily to study the generation of the seismic wave. The nature and location of the subsurface instrumentation is summarized in Fig. 15. Surface motions are planned to be measured at 47 locations, from a point 100 ft from the collar of GB-E to the rims of the San Juan Basin. Twelve of these stations are within five miles of surface ground zero, while six will measure the response of the Navajo Dam and the El Vado Dam.

NUCLEAR OPERATION

The nuclear explosive will be placed in a cylindrical canister 17 in. in diameter and 13 ft long. Part of the space in this canister is occupied by a cooling module designed to keep the temperature inside the canister below 100°F. The canister and cables are designed and tested to withstand an external pressure of over 2000 psi. When all electrical and mechanical systems have been checked, the top of the explosive canister will be attached to a 7-in. drill casing and lowered to the bottom of GB-E by a drill rig. The cables from the explosive and the shock instrumentation will be attached to this casing as it is lowered. After the lowering operation is complete, cement will be pumped into the hole to a height of 1250 ft above the canister. The balance of the hole, except for the top 50 ft, will be filled with sand. A liquid polymer that sets to a consistency of vulcanized rubber will then be pumped into the remaining space. When everything is in readiness for the detonation, an area out to a radius of 2-1/2 miles from GB-E will be cleared of personnel, and the final electrical connections will be made. An automatic 15-min countdown sequence will then be started from the timing and firing trailer at the Control Point. During this sequence a series of electrical signals will energize the instruments and start the recording systems in the recording trailers. The final signal will detonate the explosive.

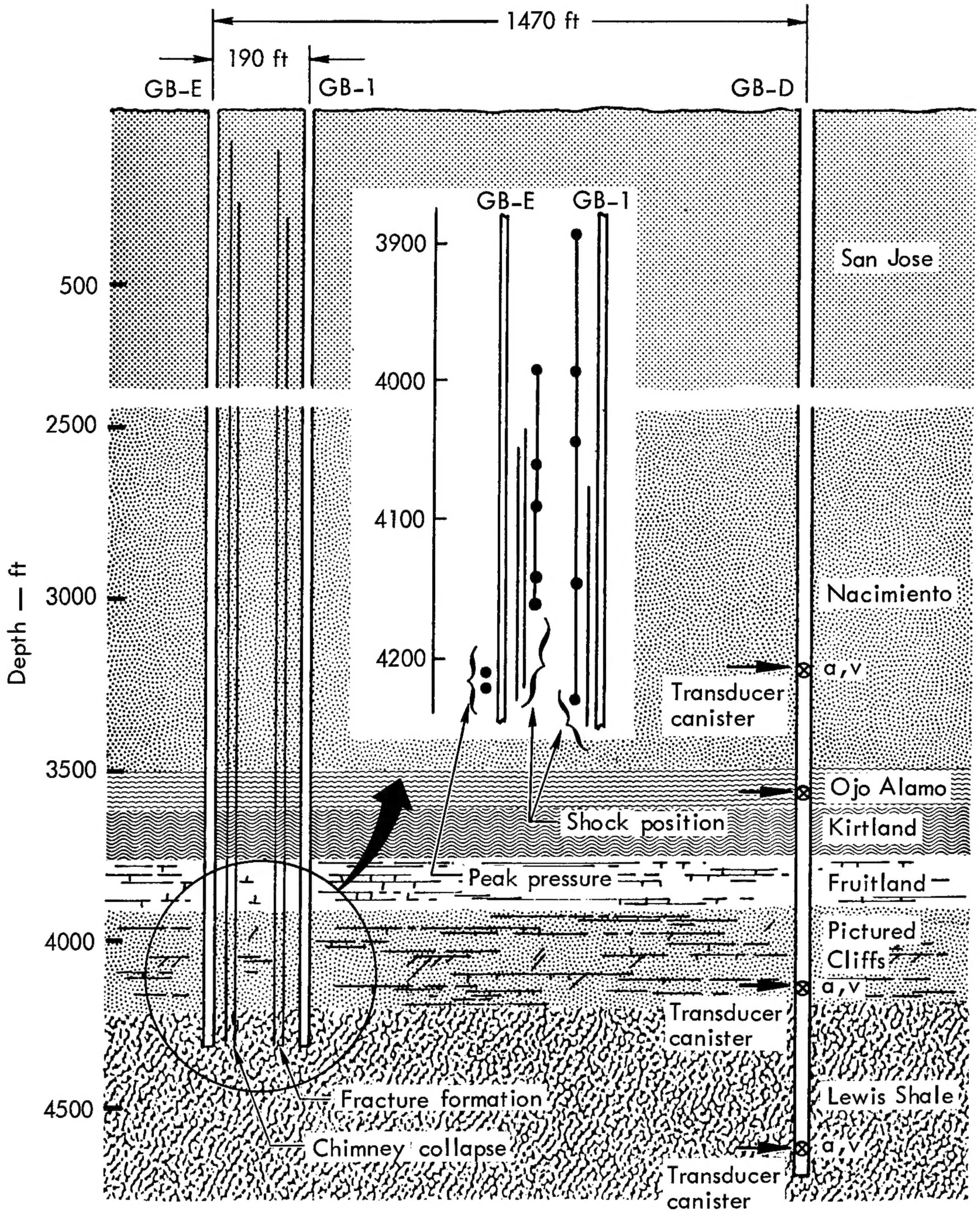

Fig. 15. Free field motion measurements.